Available online at www.sciencedirect.com
ScienceDirect
Chinese Journal of Aeronautics 21(2008) 328-334
Chinese Journal of Aeronautics
www.elsevier.com/locate/cja

Foreign Object Damage to Fan Rotor Blades of Aeroengine Part II: Numerical Simulation of Bird Impact

Guan Yupu*, Zhao Zhenhua, Chen Wei, Gao Deping

College of Energy and Power Engineering, Nanjing University of Aeronautics and Astronautics, Nanjing 210016, China

Received 30 October 2007; accepted 17 March 2008

Abstract

Bird impact is one of the most dangerous threats to flight safety. The consequences of bird impact can be severe and, therefore, the aircraft components have to be certified for a proven level of bird impact resistance before being put into service. The fan rotor blades of aeroengine are the components being easily impacted by birds. It is necessary to ensure that the fan rotor blades should have adequate resistance against the bird impact, to reduce the flying accidents caused by bird impacts. Using the contacting-impacting algorithm, the numerical simulation is carried out to simulate bird impact. A three-blade computational model is set up for the fan rotor blade having shrouds. The transient response curves of the points corresponding to measured points in experiments, displacements and equivalent stresses on the blades are obtained during the simulation. From the comparison of the transient response curves obtained from numerical simulation with that obtained from experiments, it can be found that the variations in measured points and the corresponding points of simulation are basically the same. The deforming process, the maximum displacements and the maximum equivalent stresses on blades are analyzed. The numerical simulation verifies and complements the experiment results.

Keywords: aerospace propulsion system; bird impact; numerical simulation; fan rotor blade; transient response

1 Introduction

In recent years, a novel method, the finite element numerical analysis, has been developed for the analysis of transient response of aeroengine blades impacted by birds[1-2]. The solid-solid coupling algorithm[3-5], fluid-solid non-coupling algorithm[6], fluid-solid coupling algorithm[7] and contacting-impacting algorithm[8] are the four algorithms used for this purpose, among which the contacting-impacting algorithm is the most effective algorithm. Since 1990, various kinds of algorithms based on the finite element method have been extensively used to analyze the transient response of fan blades[9-15] and compressor blades[16-18] impacted by birds. On the basis of the bird impact experiments of the fan rotor blades of the aeroengine[19], the numerical analysis for the transient response of blades impacted by bird is performed using the contacting-impacting algorithm under the experimental conditions of bird impact (such as the dimension, mass and the impacting velocity, angle and position of the analogue bird). The results of numerical simulation of all the two experiments are analyzed in this study.

2 Computational Model

The contacting-impacting algorithm and the explicit nonlinear dynamic software ANSYS/LS-DYNA are used in the numerical simulation. The fan rotor blades are mainly comprised of alloy titanium. The bilinear material model is used. The elastic modulus is 112 GPa, the density is 4 440 kg/m^3,

*Corresponding author. Tel.: +86-25-84890515.
E-mail address: ypguan@nuaa.edu.cn

the Piosson's ratio is 0.27, the yield stress is 825 MPa and the hardening modulus is 1 120 MPa. The fluid dynamic material model is used for the analogue bird. The influence of high material strain rate on the deformation of blade is ignored in this study and the computational results may lean toward safety[20].

The rheological phenomenon takes place during high velocity bird impact[21]. Generally, the strength of the material for bird can be ignored. The stress in the model of dynamic viscosity can be defined as

$$\sigma_{ij} = \mu\dot{\varepsilon}_{ij}' \tag{1}$$

where μ is the dynamic viscous coefficient of fluid material and $\dot{\varepsilon}_{ij}'$ is the deviation of strain rate. The fluid pressure of the material model during compressing is calculated using a state equation. The following Gruneisen's state equation is used in this study:

$$p = \frac{\rho_0 c^2 \eta\left[1+\left(1-\frac{\gamma_0}{2}\right)\eta-\frac{a}{2}\eta^2\right]}{\left[1-(s_1-1)\eta-s_2\frac{\eta^2}{\eta+1}-s_3\frac{\eta^3}{\eta+1}\right]^2}+(\gamma_0+a\eta)E \tag{2}$$

where c is the disconnected coefficient of voluminal stress-strain curve; s_1, s_2, and s_3 are the slope coefficients of voluminal stress-strain curve; γ_0 the Gruneisen's coefficient; a is the voluminal modified factor; $\eta = \rho_t/\rho_0 - 1$, and ρ_t the density at time t.

The impacting velocities, directions, incident angles and impacting positions are consistent with the measured values of experiments[19]. The impacting velocities and directions are taken into consideration (see Table 1). By analysis, a three-blade model is established. The blades from left to right are numbered as I, II, and III. The three-blade model can be used to simulate the experiments process well, and the complexity of the fan rotor blades can be reduced too. Through the shrouds, the blades contact each other and the impact load is transferred. The rigid bodies on the outside of blades are used to restrict the shrouds. The rabbets of blades are also restricted (see Fig.1). The mesh division is performed using Element No. 164 (8-node hexahedron). The analogue bird (cylinder) is divided into 1 014 elements. Individual blade is divided into 2 011 elements. The sum of elements for the three-blade model is 6 033. The contacts of bird with the three-blade model and blade with blade are defined. The normal contact forces are automatically exerted between all invading nodes and contact faces based on the penalty modes of contacting-impacting algorithm.

Table 1 Various calculation parameters of bird for calculation

Sample	Blade 1	Blade 2	Blade 3	Blade 4
Impact position	Mid	Tip	Mid	Tip
Deflection angle of axes/(°)	–12.40	–32.90	–8.08	–33.20
Velocity of bird /(m·s^{-1})	187.9	179.3	184.0	147.8

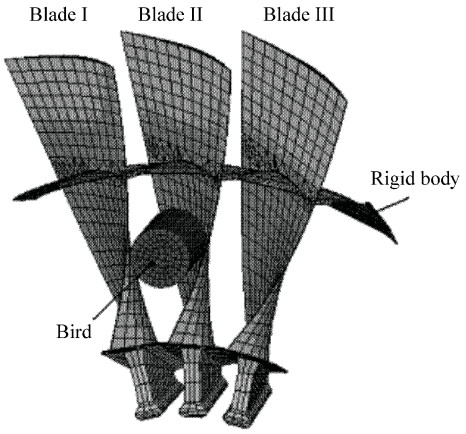

Fig.1 Three-blade model of bird impact.

3 Results of Simulation and Analysis

3.1 Blade 1

The positive voltage of the measured curves of experiments corresponds to the compressive strain. The measured curves of experiments and the calculated curves are given in Fig.2. By comparison, it is known that the variations in stretching and compressing are basically the same as shown in Fig.2(a)[19] and Fig.2(b) as well as Fig.2(c)[19] and Fig.2(d). In Fig.2, Δt is the time difference between the maximum strain and the adjacent peak strain.

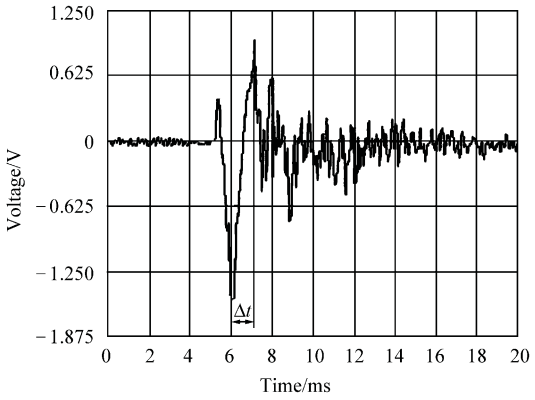

(a) Point 1 in experiment

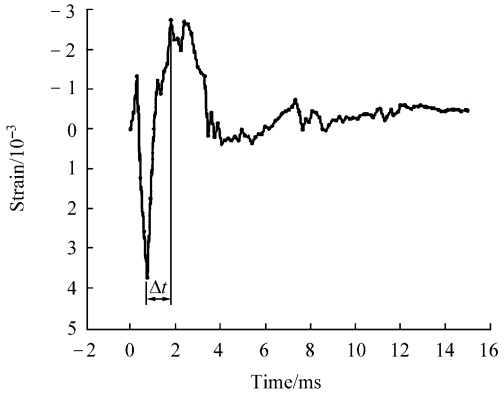

(b) Calculating point corresponding to point 1

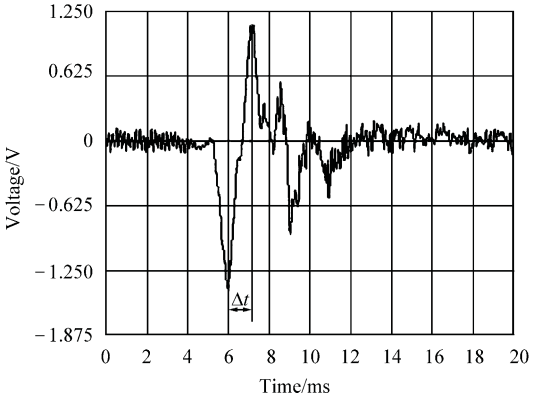

(c) Point 2 in experiment

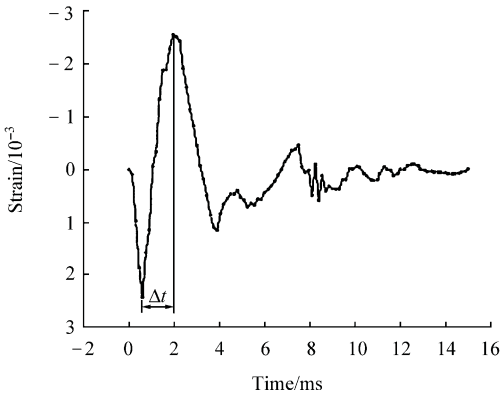

(d) Calculating point corresponding to point 2

Fig.2 Measured and calculated strain curves of Blade 1.

Equivalent stress diagrams of the three-blade model of bird impact at certain moments are given in Fig.3. When $t = 0.15$ ms, the middle portion of Blade II begins to be impacted by the bird (see Fig.3(a)). The maximum equivalent stress in the contacting area is 265 MPa. Beginning from the moment, the failed elements of bird are deleted from the contacting process. As the impact load of bird increases, a high stress area of comparatively large range becomes closer to the impact center of Blade II and the area above the shroud is affected. The impact load is continuously loaded on Blade III through the shrouds. The area of stress concentration above the shroud and a large range of high stress areas below the shroud comes closer to Blade III because of bending. When $t = 0.45$ ms, the tail of bird begins to enter the impact area (see Fig.3(b)). At the moment of $t = 0.90$ ms, the maximum equivalent stress of blades is 1 190 MPa. The stresses of the body and root of Blade II are also comparatively large (see Fig.3(c)). When the body of bird is consumed and the load is decreased, the equivalent stresses of the blades are also diminished. But Blade II is still bending toward Blade III. The body of bird is exhausted at $t = 1.35$ ms (Fig.3(d)). Because of the propagation and reflection of stress waves, the stresses and deformations, blades will

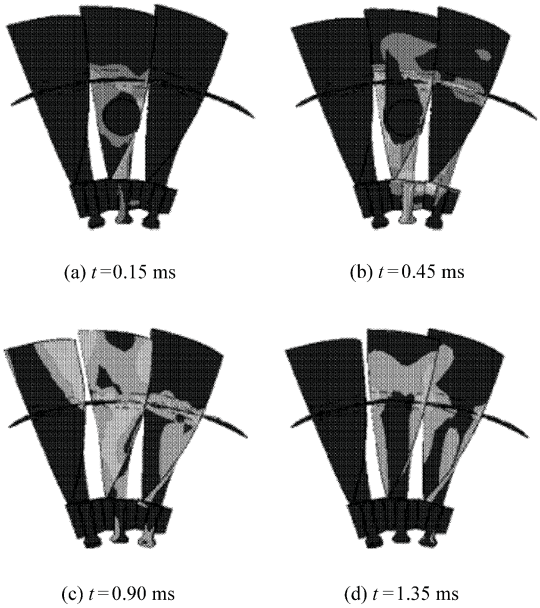

(a) t=0.15 ms (b) t=0.45 ms

(c) t=0.90 ms (d) t=1.35 ms

Fig.3 Equivalent stresses of blades.

vibrate. Along with the weakening of stress waves, the stress levels of blades go down. The stress concentrated areas are primarily located at the center of bird impact location and the contact part of shroud. The obvious plastic deforming area does not appear on the blade body.

To sum up, when the middle part of blades is impacted by bird, rheological phenomenon occurs. The stress concentration takes place at the impacted areas, the shroud and the root of blade. And the energy is transmitted between blades through the shrouds.

Displacement and stress histories of various nodes at some characteristic positions of Blade II are given in Figs.4-5. From Fig.4, it can be seen that the node displacement of x direction at the leading edge of blade tip is relatively large, and the maximum absolute value is 20.93 mm. Within the calculation time of 10 ms, there is obviously a complete vibration at the blade tip and the time interval is 5.5 ms. The node displacement in y direction is also relatively large, the maximum is 14.83 mm. During the deformation of blade, the blade tip goes toward the initial equilibrium position. It is indicated that the plastic deformation of blade is not obvious. From the equivalent stress histories of some nodes given in Fig.5, it can be seen that the stresses of the shroud slightly exceed the yield limit of material. It is clearly stated that the small areas of shroud and the shroud connecting with the blade body are slightly impacted by bird impact.

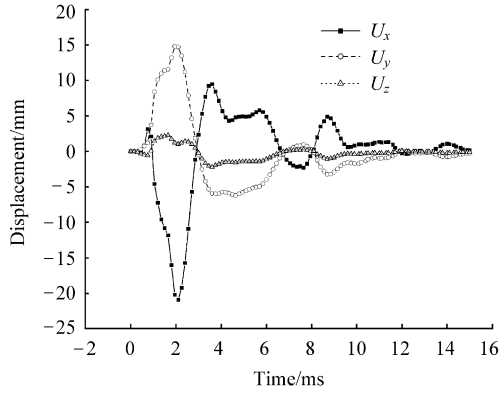

Fig.4 Displacement history of a node at blade tip.

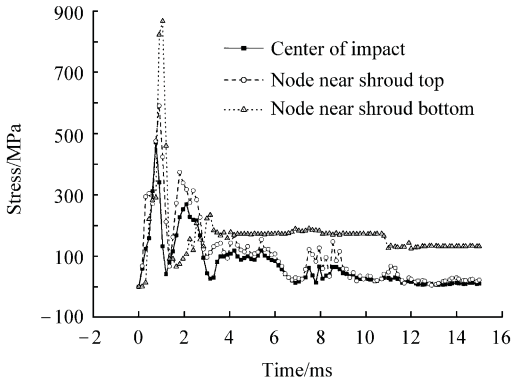

Fig.5 Equivalent stress histories of some nodes on Blade II.

3.2 Blade 4

The measured curves of experiments and the calculated curves are given in Fig.6. By comparison, it can be seen that the variations in stretching and compressing are the same.

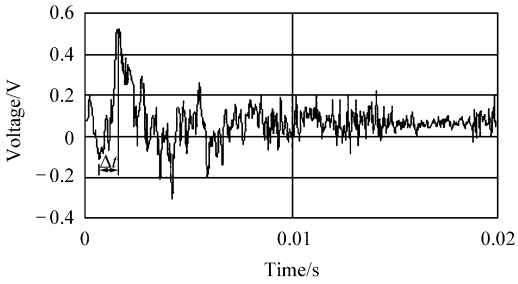

(a) Point 1 in experiment

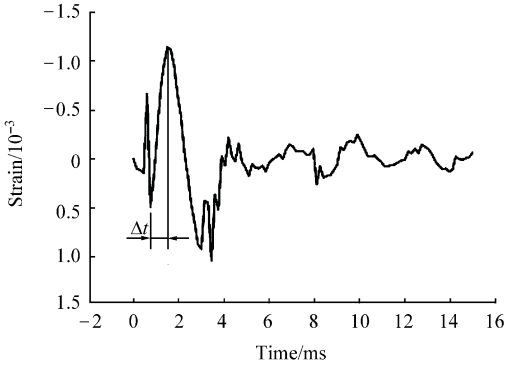

(b) Calculating point corresponding to point 1

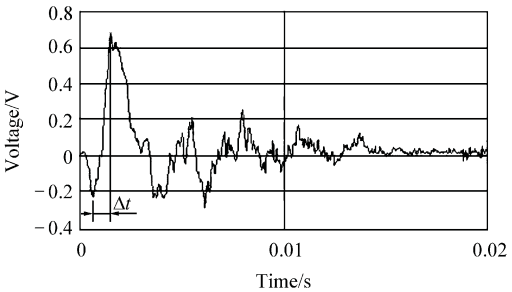

(c) Point 2 in experiment

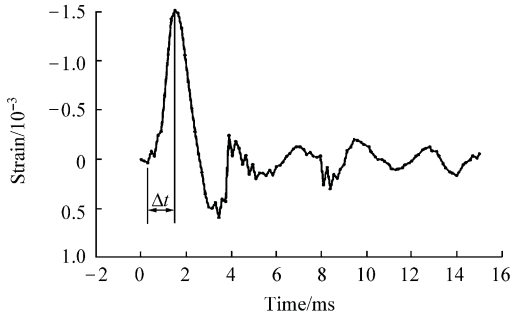

(d) Calculating point corresponding to point 2

Fig.6 Measured and calculated strain curves of Blade 4.

Equivalent stress diagrams for the three-blade model of bird impact at certain moments are given in Fig.7. The tip of Blade II is impacted by the bird. When the bird comes closer to Blade II, the stresses within the contact area rapidly increases. Because of the deformation of Blade II, the contacting area between Blade II and Blade III becomes small and the contacting stress reaches 538 MPa at $t = 0.45$ ms (see Fig.7(a)). As the impact load of bird increases, there is comparatively a large scope for the generation of high stress area at the impact center and adjacent area of the shroud of Blade II, and the blade edge under the shroud is influenced. The impact load is continuously loaded on Blade III through the shroud. The areas of stress concentration are generated on the shroud and its nearby area of Blade III. When $t = 0.75$ ms, the tail of bird begins to enter the impact area. The maximum stress of the blades is 1 020 MPa. The stresses of the impact area and the edge under the shroud of Blade II are also comparatively large (see Fig.7(b)). As the body of bird is consumed and the load is decreased, Blade II is still bended toward the direction of Blade III. When $t = 1.65$ ms, the body of bird is exhausted and the maximum stress is 783 MPa (see Fig.7(c)). Because of the propagation and reflection of stress waves, the stresses of Blades II and III as well as the two blades appear as oscillations. At $t = 3.90$ ms, the shrouds of Blades I and II contact each other. The comparatively large stresses appear near both shrouds. The maximum stress is 848 MPa (see Fig.7(d)). As the blades are vibrating and the stress waves are weakened, the stress levels of the blades are decreased. The areas of stress concentration are primarily located at the center of the bird impact areas and the contacting part of the shroud. The area with obvious plastic deformation does not appear on the blade body.

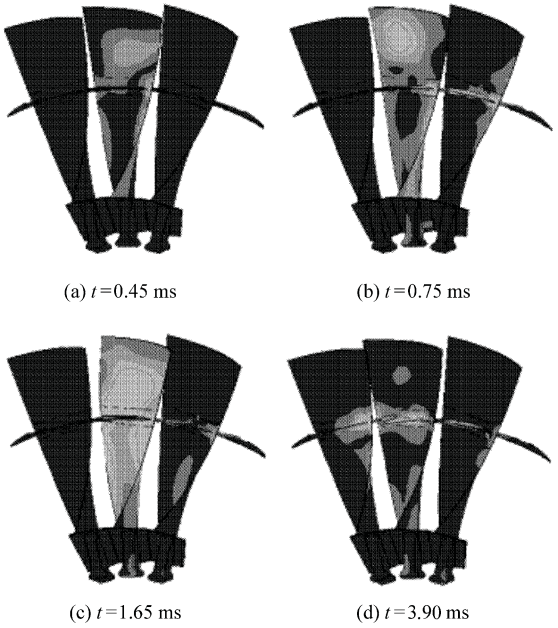

(a) $t = 0.45$ ms (b) $t = 0.75$ ms

(c) $t = 1.65$ ms (d) $t = 3.90$ ms

Fig.7 Equivalent stresses of blades under bird impact.

The displacement and stress histories of several nodes at certain specific positions of Blade II are given in Figs.8-9. From Fig.8, it can be seen that the node displacement along x direction is relatively large on the leading edge of blade tip, the maximum absolute value is 19.28 mm. Within 10 ms of calculation time, a complete vibration occurs on the blade tip. The time interval is 9 ms. The node displacement along y direction is also relatively large, the

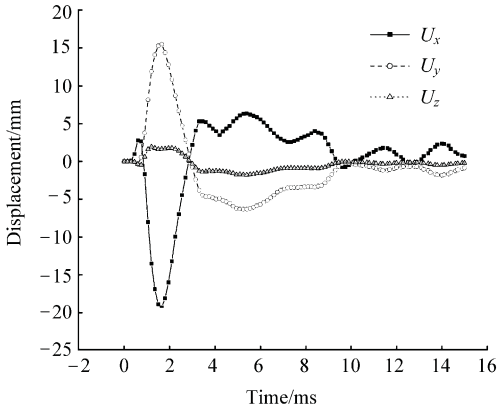

Fig.8 Displacement history of a node at blade tip.

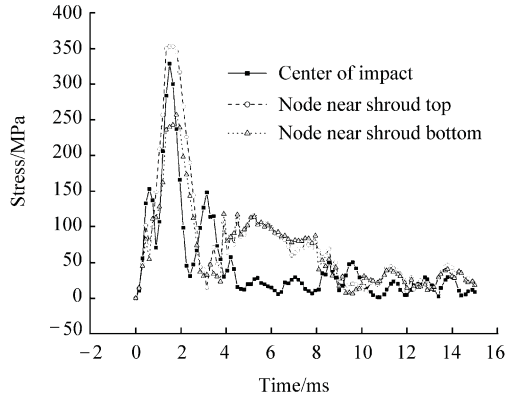

Fig.9 Equivalent stress histories of some nodes on Blade II.

maximum is 15.49 mm. In the course of the deformation of blade, the blade tip tends the initial equilibrium position. It is indicated that the plastic deformation of the blade is not obvious. From the equivalent stress histories of certain nodes in Fig.9, it is clear that the stresses of the impact center and the parts joined with shrouds of the blade body do not exceed the yield limit of material.

In Table 2, comparison of the maximum strains of measured and calculated points of Blade 1 and Blade 4 is provided. Blade 1 has the maximum stretching strains and Blade 4 has the maximum compressing strains. Because of the use of 8-node hexahedrons and the location of calculated strain at the integral point, the absolute values of the maximum and the minimum relative errors between the measured maximum strain and the calculated maximum strain are 31.05% and 1.06%, respectively.

Table 2 Comparison of maximum strains between measured and calculated points

Sample		Blade 1			Blade 4		
		Experiment	Simulation	Relative error/%	Experiment	Simulation	Relative error/%
Point 1	Δt/ms	1.03	1.04	0.97	0.93	0.77	–17.20
	ε_{max}/‰	3.78	3.74	–1.06	–0.96	–1.15	19.79
Point 2	Δt/ms	1.13	1.33	17.70	0.88	1.18	34.09
	ε_{max}/‰	3.51	2.42	–31.05	–1.19	–1.51	26.89

4 Conclusions

Using the numerical computation method, the transient responses of fan rotor blades impacted by bird under experimental conditions are simulated. The conclusions drawn through analysis are summarized as follows:

(1) The contacting-impacting algorithm can be used to better simulate the process of blades impacted by the analogue bird.

(2) The model of dynamic viscosity is appropriate to represent the dynamic characteristics of the analogue bird under impacting loads during experiments.

(3) The impacting damage of blades caused by the bird impact on the tip of blades is more severe than that on the middle of blades.

(4) The numerical simulation provides more results than experiments. The numerical simulation can be exploited to verify and complement experiment results.

References

[1] Chen W, Guan Y P, Gao D P. Numerical simulation of the transient response of blade due to bird impact. Acta Aeronautica et Astronautica Sinica 2003; 24(6): 531-533. [in Chinese]

[2] Guan Y P, Chen W, Gao D P. Present status of investigation of foreign object damage to blade in aeroengine. Acta Aeronautica et Astronautica Sinica 2007; 28(4): 851-857. [in Chinese]

[3] Johson G R. Analysis of elastic-plastic impact inviting severe distortion. Journal of Applied Mechanics 1976; (9): 439-443.

[4] Johson G R. High velocity impact calculation in three dimensions. Journal of Applied Mechanics 1977; 44(1): 95-100.

[5] Walsh R T, Chou P C, Hopkins A K. Dynamic response of material to intense impulsive loading. Wright Patterson AFB, OH: Air Force Materials Laboratory, 1972; 363-403.

[6] Fan E N. Investigation for load and transient response of blades impacted by birds in engines. MD thesis, Nanjing: Nanjing Institute of Aeronautics, 1990. [in Chinese]

[7] Nimmer R P, Boehman L. Transient, nonlinear response analysis of soft bodies impact on flat plates include interactive load deter-

mination. AIAA-81-0621, 1981.

[8] Belytschko T, Liu W K, Moran B. Nonlinear finite elements for continua and structures. New York: John Wiley & Sons Inc, 2000.

[9] Martin N F, Jr. Nonlinear finite-element analysis to predict fan-blade damage due to soft-body impact. Journal of Propulsion and Power 1990; 6(4): 445-450.

[10] Teichman H C, Tadros R N. Analytical and experimental simulation of fan blade behavior and damage under bird impact. Journal of Engineering for Gas Turbines and Power Transactions of the ASME 1991; 113(4): 582-594.

[11] Toshio M, Hidehito O, Kunihiko O. Analysis of the effect of centrifugal force on the impact resistance of composite fan blades for turbo-fan engine. Proceeding–Society of Automotive Engineers. 1991; (NP-246): 619-626.

[12] Stoll F, Brockman R A. Finite element simulation of high-speed soft-body impacts. Collection of Technical Papers–AIAA/ASME/ASCE/AHS/ASC Structures, Structural Dynamics & Materials Conference. 1997; 334-344.

[13] Imrequn M, Vahdati M. Aeroelasticity analysis of a bird-damaged fan assembly using a large numerical model. Aeronautical Journal 1999; 103(1030): 569-578.

[14] Kim M, Vahdati M, Imrequn M. Aeroelastic stability analysis of a bird-damaged aeroengine fan assembly. Aerospace Science and Technology 2001; 5(7): 469-482.

[15] Kazuo S, Tadashi S, Donald G J. Numerical simulation of bird strike damage on jet engine fan blade. American Society of Mechanical Engineers, Pressure Vessels and Piping Division (Publication) PVP–Emerging Technology in Fluids, Structures, and Fluid-Structure Interactions 2004. 2004; 485(part1): 161-166.

[16] Schuette W. Blade behaviour during birdstrike. Science and Engineering on Supercomputers. Proceedings of the Fifth International Conference. 1990; 145-157.

[17] Chen W. Analysis and experiment technique on the response of real blades due to bird impact. PhD thesis, Nanjing: Nanjing University of Aeronatics and Astronautics, 1995. [in Chinese]

[18] Menouillard T, Rethore J, Bunq H, et al. Composite blade damaging under impact. Journal de Physique IV 2006; 134(7): 409-415. [in Anglais]

[19] Guan Y P, Zhao Z H, Chen W, et al. Foreign object damage to fan rotor blades of aeroengine, part I: experimental study of bird impact. Chinese Journal of Aeronautics 2007; 20(5): 408-414.

[20] Chen W, Wen W D, Gao D P. A study on the transient response of blade under different strain rates. Journal of Nanjing University of Aeronautics and Astronautics 1998; 30(1): 96-99. [in Chinese]

[21] Wilbeck J S. Impact behavior of low strength projectiles. AFML-TR-77-134, 1978.

Biographies:

Guan Yupu Born in 1956, he received B.S. and M.S. from Jilin University of Technology (JUT) in 1982 and 1986, respectively. In 1992 he received his Ph.D. from Dalian University of Technology (DUT). He became a teacher in 1982. Since then, he has been doing research works in JUT, DUT, Shanghai Jiaotong University, and Nanjing University of Aeronautics and Astronautics. His research interests are the computational structural mechanics and structure, strength and vibration of aeroengine. He has published some scientific papers in various periodicals.
E-mail: ypguan@nuaa.edu.cn

Zhao Zhenhua Born in 1979, currently he is a Ph.D. candidate in Nanjing University of Aeronautics and Astronautics. His research interests are structure, strength and vibration of aeroengine.

Chen Wei Born in 1968, he is a professor in Nanjing University of Aeronautics and Astronautics (NUAA). He received his B.S. and Ph.D. from NUAA in 1990 and 1995, respectively. His research interests are structure, strength, vibration and reliability of aeroengine.

Gao Deping Born in 1938, he is a professor in Nanjing University of Aeronautics and Astronautics. His research interests include the structure, strength and vibration of aeroengine.